

ОБЪЕДИНЕННЫЙ  
ИНСТИТУТ  
ЯДЕРНЫХ  
ИССЛЕДОВАНИЙ  
ДУБНА

*RU9401538*

E4-93-60

M.Kh.Khankhasayev, H.Sarafian<sup>1</sup>, Mikkell B.Johnson<sup>2</sup>,  
Zh.B.Kurmanov

EFFECT OF PION EXTERNAL DISTORTION  
ON LOW ENERGY PION  
DOUBLE-CHARGE-EXCHANGE

Submitted to «Physical Review C»

<sup>1</sup>Department of Physics, Pennsylvania State University,  
York, Pennsylvania 17403, USA

<sup>2</sup>Los Alamos National Laboratory, Los Alamos,  
New Mexico 87545, USA

# 1 Introduction

In recent years, the pion-nucleus double-charge-exchange (DCX) to the double isobaric analog state (DIAS) at low energies ( $T=50$  MeV) has systematically been studied [1]-[4]. Specially at low energies this reaction attracted a lot of interest. This is because in comparison to resonance region, where pions due to the strong interaction mostly get scattered by the surface of the nuclei, here rather weak  $\pi - N$  interaction allows a deep penetration. The latter provides a useful mean to probe the nuclear interior. Moreover, because the pion changes its charge by two units, it should therefore interact with at least two nucleons. Hence the penetrability of a low energy pion on one hand and its two-body interactive character on the other provides an excellent ground to extract information on interesting topics such as: dynamical short range correlation of nucleons, isospin triplet coupling of nucleon pairs among others.

Globally there are two singular characteristics associated with the low energy pion DCX to DIAS. In the first, the magnitude of the measured cross-sections are comparable to those at resonance region. In the second, the differential cross-section is forward peaked. There are a number of proposed microscopic mechanisms in attempt to describe these features [4]-[16].

Many theoretical efforts have been devoted to clarify the role of the conventional sequential mechanism (SEQ- $\pi$ ), when two successive single-charge scattering of a pion by two nucleons takes place [5]-[9]. One can summarize the results for SEQ- $\pi$  mechanism calculated in the plane wave approximation as follows: (a) The calculated differential cross sections reproduce qualitatively the angular distributions and underestimate them by more than a factor two. Only in [7] a quantitative description of the DCX scattering data in the plane wave approximation has been obtained. (b) The plane wave results for SEQ- $\pi$  are very sensitive to the nuclear structure [6], [5], to the short range correlation effects [5], to the range of the pion-nucleon form factors [5], [8] and to uncertainties in the  $\Delta$ -N interaction [5] (especially within the framework of the  $\Delta$ -hole model [6]).

In a number of attempts it has been shown that there could be a significant contribution to the DCX via non-conventional mechanisms such as: 1) Meson-Exchange-Currents (MEC) [12], [13] and 2) Absorption channel [10], [11]. According to these reports each one of these individual "exotic" mechanisms at low energies could constructively interfere with the standard (SEQ) process and could produce almost perfect fits to the experimental DCX angular distributions. It should be stressed that these results have been obtained in the plane wave approximation and hence should not be compared to data.

The effect of a pion distortion for the SEQ- $\pi$  mechanism has been studied in several papers [4], [6]-[9]. The pion distortion comes about both from the distortion of in- and out-going pion (external distortion) as well as from the distortion of intermediate pion (internal distortion). In the Bleszynsky-Glauber paper [7] it has been noted that the pion distortion effect at low energies is of no importance and can be neglected. A strong pion distortion effect (external + internal) has been found in [6] and [4]. In the last two papers, by turning on the pion distortion, the plane wave results are magnified by a factor of two. In these papers also it has been pointed out that the main effect comes from the distortion of the intermediate pion. Turning off the internal distortion

decreases strongly the cross section. On the other hand in [9] it has been noted that the inclusion of the internal distortion generally decreases the calculated cross sections. The effect of external distortion within the framework of the DWIA-approximation has been studied recently in [8] and authors claimed that the distortion of the external pion considerably changes the plane wave angular distribution, increasing the cross sections at forward angles and decreasing them at large angles.

From the above it follows so far that the situation with the pion distortion effect is controversial and there is a need for further investigations. Taking into account that, first, the DWIA calculations are a very time consuming procedure and, second, there are several competing dynamical mechanisms, which might contribute to DCX at low energies, it is advantageous to develop an effective approximate method to take into account the pion distortion effects.

Therefore we studied the distortion problem from two different directions. 1) The intermediate distortion, which is under investigation and the results will be reported later. 2) The external distortion, which is the subject of this paper. It is very important to treat the external distortion separately. This is because for non-conventional, "exotic" mechanisms only external pions can be distorted.

The purpose of this paper is, therefore, to characterize the contribution of the pion external distortion to pion double charge exchange. We have considered this problem within the framework of the optical model, in which pion-nucleus single and double charge exchange to isobaric analog states, as well as elastic scattering, are related to the strong interaction through isospin symmetry [14-16]. The isoscalar and isovector terms of the optical potential are taken to be known and well-reproduce elastic and SCX to isobaric analog states.

In this theory, the DCX amplitude to DIAS consists of two pieces. The first contribution arises from the iteration of the isovector potential  $U_1$ , representing DCX mediated by a scattered pion and the nucleus excited to the isobaric analog state. In many cases this piece (called the analog route (AR)) is quite large and is tightly constrained by both empirical and theoretical considerations. We take our model of the analog route from Ref. [16], where the isovector interaction includes not only a lowest-order piece built up in the standard way from the free pion-nucleon scattering amplitude, but also a second-order piece representing short-range and Pauli correlations.

The second contribution to DCX comes from all other sources, including excitation of the nucleus through nonanalog-route (NAR) intermediate states and excitation of the meson and baryon fields themselves. These are represented by an isotensor term  $U_2$  in the optical potential. It consists of a coherent sum of plane-wave amplitudes for the corresponding phenomena, including (among others) DCX mediated by pion absorption channels ( $U_2^{obs}$ ), by meson exchange currents ( $U_2^{MEC}$ ), and by nonanalog nuclear states ( $U_2^{NAR}$ ). One of the ultimate goals is to use measurements of DCX as a mean for quantitatively testing models of the isotensor interaction. We will illustrate our method of including external distortions using only one piece of the complete isotensor interaction, namely  $U_2^{NAR}$ , which is constructed from the SEQ mechanism taken from Ref. [5]. This is built up from excitation of the nucleus to all intermediate states and includes the effects of short-range nucleon-nucleon correlations and an intermediate rho meson. Details of constructing the isotensor potential  $U_2^{NAR}$  are discussed in Appendix A, where, first of all, an isotensor potential  $U_2^{SEQ}$  is formed from the SEQ model of

Ref. [5] and, secondly, the contributions from analog states,  $\Delta U^{AR}$ , are subtracted to avoid double counting with the analog route taken from the theory of Ref. [16],

$$U_2^{NAR} \equiv U_2^{SEQ} - \Delta U_2^{AR}.$$

Later, in Sect. 4, we compare  $\Delta U_2^{AR}$  with the analog-route contributions obtained from Ref. [16] to get the differences reflecting the importance of medium modifications (second-order effects) in  $U_1$ .

To calculate the distorted wave (DW) amplitude we have developed a procedure based on the approximating the given optical potential with a separable interaction. This makes it possible to present the DW amplitude as a product of the plane wave (PW) amplitude and the distortion factor at the given partial channel. These distortion factors are expressed in terms of the pion-nucleus form factors, which determine the off-energy-shell behavior of the elastic scattering amplitude. We obtain the  $\pi$ -nucleus form factors using the Bateman separable approximation method [22].

This paper is organized as follows. In section 2, we present the general formalism within the framework of the isospin invariant model: the two potential formulas for the DCX amplitude is derived and an expression for the DW-amplitude in the separable approximation is obtained. The section 3 is devoted to the calculation of the  $\pi$ -nucleus form factors. In section 4 we present results and conclusions. In Appendix A the details of constructing the isotensor potential  $U_2^{SEQ}$  and in Appendix B the details concerning the procedure of calculation the  $\pi$ -nucleus form factors are given.

## 2 Formalism

### 2.1 Isospin-Invariant Optical Model

Pion-nucleus isoelastic scattering (if we assume that isospin breaking effects can be ignored) can be treated theoretically on the basis of an optical potential of the form

$$\hat{U} = U_0 + U_1(\vec{\phi} \cdot \vec{T}) + U_2(\vec{\phi} \cdot \vec{T})^2 \quad (1)$$

where the  $\vec{\phi}(\vec{T})$  is the pion (nucleus) isospin operator [14]. We assume that the isoscalar ( $U_0$ ) and isovector ( $U_1$ ) potentials are known and are fitted to the elastic and single-charge exchange data [14], [15], [16]. The isotensor potential ( $U_2$ ) doesn't contribute significantly to the elastic and SCX channels, but dominates in the DCX. The  $\pi$ -nucleus scattering T-matrix has the identical isospin structure:

$$\hat{T} = T_0 + T_1(\vec{\phi} \cdot \vec{T}) + T_2(\vec{\phi} \cdot \vec{T})^2 \quad (2)$$

The DCX scattering amplitude is determined through the isotensor term as

$$\langle \pi^-; DIAS | \hat{T} | \pi^+; g.s. \rangle = \sqrt{T_0(2T_0 - 1)} T_2, \quad (3)$$

where  $T_0$  is the z-component of the nuclear isospin;  $T_0 = (N - Z)/2$ ,  $|g.s.\rangle = |T_0, -T_0\rangle$  and  $|DIAS\rangle = |T_0, -T_0 + 2\rangle$ . The plane-wave Born approximation (PWBA) for  $T_2$  is

$$T_2^{PWBA} = \langle \pi^-; DIAS | U_2 | \pi^+; g.s. \rangle \quad (4)$$

In recent years many theoretical efforts [3]-[16] were directed toward different mechanisms contributing to  $U_2$ . In the present paper we are interested in the calculation of the effect of external pion distortion on the plane-wave results within the framework of the optical model.

## 2.2 Two-potential Formalism

Let us represent the optical potential Eq.(1) in the following form

$$\hat{U} = \hat{V} + \hat{R} \quad (5)$$

where

$$\hat{V} = U_0 + U_1(\vec{\phi} \cdot \vec{T}) \quad (6)$$

$$\hat{R} = U_2(\vec{\phi} \cdot \vec{T})^2 \quad (7)$$

Since  $U_2 \ll U_1 \ll U_0$  [16], the isotensor term  $U_2$  could be considered as a perturbation to the elastic and SCX channels. Therefore within the framework of the two-potential formalism [17] we obtain the following expression for the total scattering matrix

$$T = T_V + \Omega_V^{(-)+} [\hat{R} + \hat{R} G_P^{(+)} \hat{R}] \Omega_V^{(+)} \quad (8)$$

where  $G_P^{(+)}$  is a full Green function

$$G_P^{(+)} = [E - \mathcal{H} \pm i\delta]^{-1}, \quad (9)$$

for the Hamiltonian

$$\mathcal{H} = K_\pi + H_A + \hat{U}. \quad (10)$$

Here  $T_V$  is a scattering matrix and  $\Omega_V^{(\pm)}$  is a Möller operator for the Hamiltonian

$$\mathcal{H}_V = K_\pi + H_A + \hat{V}, \quad (11)$$

where  $K_\pi$  is a pion kinetic energy operator,  $H_A$  is the nuclear Hamiltonian and  $V$  is given by Eq.(6). The Möller operator is expressed in terms of the  $T_V$ -matrix as:

$$\Omega_V^{(\pm)} = 1 + \hat{P} G^{(\pm)} T_V^{(\pm)}, \quad (12)$$

where  $G^{(\pm)}$  is a free Green function

$$G^{(\pm)}(E) = (E - K_\pi - H_A \pm i\delta)^{-1} \quad (13)$$

and  $\hat{P} = |0\rangle\langle 0|$  is a projection operator into the nuclear isobar analog states (ground states).

For DCX scattering to DIAS we get

$$\langle \pi^-; DIAS | T | \pi^+; g.s. \rangle = T_V^{AR} + \sqrt{T_0(2T_0 - 1)} T_2^{DWBA} \quad (14)$$

Here  $T_2^{AR}$  is the contribution to DCX through the analog route transitions (at least two actions of the isovector potential). If we neglect in Eq.(7) with the higher order terms in  $\sim \hat{R}$  we are getting the distorted wave Born approximation (DWBA) for the isosensor amplitude, where

$$T_2^{DWBA} = \langle \psi_{\vec{k}_f}^{(-)}(\pi^-; DIAS) | U_2 | \psi_{\vec{k}_i}^{(+)}(\pi^+; g.s.) \rangle \quad (15)$$

here

$$\psi_{\vec{k}}^{(\pm)} = \Omega_V^{(\pm)} | \vec{k} \rangle \quad (16)$$

From Eqs. (14) and (16) it follows that the procedure of taking into account the pion distortion consists of (a) replacing the pion plane-waves in Eq.(4) by the distorted waves, and (b) adding the term  $T^{AR}$ , which describes the contribution to DCX through the analog route transitions.

### 2.3 Distortion Factors

Introducing in Eq.(15) a complete set of intermediate pion-nucleus plane-wave states one can rewrite Eq.(15) in the following form:

$$T_2^{DWBA}(E) = \sum_{\vec{q}_1, \vec{q}_2} D_{\pi^-, DIAS}^{(-)}(\vec{k}_f, \vec{q}_1; E) \langle \pi^-, \vec{q}_1; DIAS | T_2^{PWBA}(E) | \pi^+, \vec{q}_2; g.s. \rangle \times D_{\pi^+, g.s.}^{(+)}(\vec{q}_2, \vec{k}_i; E) \quad (17)$$

where the distortion factors  $D^{(\pm)}$  are defined by

$$D^{(\pm)}(\vec{k}, \vec{q}; E) \equiv \langle \vec{k} | \Omega_V^{(\pm)}(E) | \vec{q} \rangle = (2\pi)^3 \delta(\vec{k} - \vec{q}) + T_V^{(\pm)}(\vec{k}, \vec{q}; E) \frac{1}{E - E(q) \pm i\delta} \quad (18)$$

The sum over  $q_1$  and  $q_2$  is

$$\sum_{\vec{q}_1, \vec{q}_2} \equiv \int \frac{d\vec{q}_1}{(2\pi)^3} \int \frac{d\vec{q}_2}{(2\pi)^3}$$

and  $E = E(k_f) = E(k_i)$  is the scattering energy. In Eq.(17) we neglected the small contributions, which might come from the single isobaric analog intermediate states.  $T_V^{(\pm)}$  in Eq.(18) are the elastic pion scattering amplitudes in the initial and final channels. For nuclei such as:  $^{14}\text{C}$ ,  $^{18}\text{O}$ , which have the isospin  $T_0 = 1$ , one may realize that by ignoring the Coulomb potential the distortion factors of initial and final states could be identical and, therefore,

$$D_{\pi^-, DIAS}^{(\pm)} = D_{\pi^+, g.s.}^{(\pm)} \quad (19)$$

## 2.4 Partial Wave Expansion

Let us decompose all quantities in Eq.(17) into the partial wave series

$$\langle \vec{k} | \hat{O}(E) | \vec{q} \rangle = 4\pi \sum_{\alpha} \bar{Y}_{\alpha}(\vec{k}) \mathcal{Y}_{\alpha}(\vec{q}) O_{\alpha}(k, q), \quad (20)$$

where  $\alpha$  denotes the quantum numbers of a given partial channel such as: the orbital angular momentum (l), total angular momentum (I), isospin (T), etc. To simplify formulation we consider the case of the spinless nuclei having isospin  $T_0 = 1$ . In this case  $\alpha = (l, I)$ , where  $I = T_0 \pm 1, T_0$ . For the partial wave of  $T_2^{DWBA}$  we obtain

$$T_{2,\alpha}^{DWBA}(E) = \int_0^{\infty} \frac{q_1^2 dq_1}{2\pi^2} \int_0^{\infty} \frac{q_2^2 dq_2}{2\pi^2} D_{\alpha}^{(-)\dagger}(k_f, q_1; E) T_{2,\alpha}^{PWBA}(q_1, q_2; E) D_{\alpha}^{(+)}(q_2, k_i; E) \quad (21)$$

where the partial components of the distortion factors are:

$$D_{\alpha}^{(\pm)}(k, q; E) = 2\pi^2/k^2 \delta(k - q) + T_{\alpha}^{(\pm)}(k, q; E) \frac{1}{E - E(q) \pm i\delta} \quad (22)$$

Note that for the isoelastic scattering ( $k_f = k_i$ ) there is the identity:

$$D_{\alpha}^{(-)\dagger}(k, q; E) = D_{\alpha}^{(+)}(q, k; E) \quad (23)$$

## 2.5 On-Shell Distortion Factor

If we neglect in Eq.(22) the off-energy shell part of the Green function by combining the on-energy shell of Eq.(22) with (21) and integrating over the  $q_1$  and  $q_2$  we get

$$T_{2,\alpha}^{DWBA}(k_f, k_i; \text{on-shell}) = \tilde{\gamma}_{\alpha}^{DW}(k_f, k_i) T_{2,\alpha}^{PWBA}(k_f, k_i; E(k)) \quad (24)$$

where the distortion factor  $\tilde{\gamma}(k_f, k_i)$  is defined by:

$$\tilde{\gamma}_{\alpha}^{DW}(k_f, k_i; \text{on-shell}) = (1 + ik_f F_{\alpha}(k_f))(1 + ik_i F_{\alpha}(k_i)) \quad (25)$$

Here  $F_{\alpha}(k)$  is the  $\pi$ -nucleus elastic scattering amplitude given by:

$$F_{\alpha}(k) = -\frac{\bar{\omega}}{2\pi} T_{\alpha}^{(+)}(k, k; E(k)), \quad (26)$$

where  $\bar{\omega}$  is the reduced pion-nucleus mass.

## 2.6 Off-shell Distortion Factors

The most difficulty comes from the problem of taking into account the effects of the off-energy shell pion distortion, which is related to the principle value integration in Eq.(22). We use an approach based on the approximating the given optical potential with the separable interaction. Here we use the rank-one separable potential. Within the framework of this model the off-shell T-matrix is expressed in terms of the on-shell scattering matrix

$$T_{\alpha}(q_1, q_2; E) = T_{\alpha}(k, k; E(k)) \frac{g_{\alpha}(q_1)g_{\alpha}(q_2)}{g_{\alpha}^2(k)} \quad (27)$$

Here the  $g(q)$  is the pion-nucleus form factor defined in Sect. 3. It is also natural to assume that identical form factor could be used for the off-shell behavior of the plane-wave amplitude in Eq.(21). Using Eq.(27) we obtain

$$T_{2,\alpha}^{DWBA}(k_f, k_i; E) = \gamma_{\alpha}^{DW}(k_f, k_i) T_{2,\alpha}^{PWBA}(k_f, k_i; E), \quad (28)$$

where

$$\gamma_{\alpha}^{DW}(k_f, k_i) = (1 - k_f F_{\alpha}(k_f) \xi_{\alpha}(k_f))(1 - k_i F_{\alpha}(k_i) \xi_{\alpha}(k_i)) \quad (29)$$

and

$$\xi_{\alpha}(k) = \frac{1}{\pi \epsilon_{\pi A}(k)} \int_0^{\infty} \frac{q^2 dq}{2\pi^2} \left[ \frac{g_{\alpha}(q)}{g_{\alpha}(k)} \right]^2 \frac{1}{E(k) - E(q) + i\delta} \quad (30)$$

Here  $\epsilon_{\pi A}(k) = k^2/[2\pi^2 dE(k)/dk] = k\bar{\omega}/2\pi^2$  is the scattered states density. For the isoelastic scattering  $k_i = k_f$ . If we neglect the principle value part of the integral in Eq.(30), the distortion factor (29) could be reduced to the on-shell result given by Eq.(25).

### 3 Pion-Nucleus Form Factor

In this section we outline the procedure of determining the  $\pi - A$  form factor following Bateman method [22]. This method is based on an assumption that at low energies the  $\pi - A$  elastic scattering could be analyzed in terms of a separable rank-one potential.

There are a number of different optical potentials, which equally well describes the low energy  $\pi - A$  interaction [18]-[21]. It has been shown yet [19] that all these potentials are closely related to Kisslinger potential. This globally parameterized potential is given by

$$\frac{-2\bar{\omega}}{4\pi} U(r) = b_{eff} \rho(r) - c_{eff} \bar{\nabla} \rho(r) \bar{\nabla} + c_{eff} \frac{\bar{\omega}}{2M} \bar{\nabla}^2 \rho(r) \quad (31)$$

where  $\bar{\omega}$  is the  $\pi - A$  reduced mass,  $\rho(r)$  is the nuclear density, and  $b_{eff}$  and  $c_{eff}$  are the complex energy dependent parameters. To apply the separable approximation method following Bateman, momentum space representation of this potential is decomposed in the partial waves. So, a partial wave component of the rank-one potential is given by:

$$V_L(k', k) = V_L^{(1)}(k', k) = \lim_{s \rightarrow 0} \frac{V_L(k', s) V_L(s, k)}{V_L(s, s)} \quad (32)$$

It is shown in Appendix B that Eq.(32) leads for the  $\pi - A$  optical potential given in Eq.(31) to the following  $\pi$ -nucleus form factors

$$g_L(k) = k^L e^{-k^2/4\alpha} (1 - \beta_1 \frac{k^2}{4\alpha} - \beta_2 (\frac{k^2}{4\alpha})^2) \quad (33)$$

where

$$\begin{aligned}\beta_1 &= [w(1 + L\eta) - 2\epsilon R(1 + w(L + \frac{3}{2}))]/D_L \\ \beta_2 &= 2w\epsilon R/D_L \\ D_L &= 1 + L\eta + w(L + \frac{3}{2})(1 + \frac{L(2L+1)}{2L+3}\eta) \\ \eta &= 2(1 - \epsilon)R\end{aligned}\quad (34)$$

Here  $\epsilon = \bar{\omega}/M$ ,  $M$  is the mass of the nucleon,  $R = \alpha c_{eff}/b_{eff}$ , where  $\alpha$  and  $w$  are the parameters determining the nuclear matter density, which is taken in the form

$$\rho(r) = \rho_0(1 + w\alpha r^2)\exp(-\alpha r^2) \quad (35)$$

## 4 Numerical Calculations, Results and Conclusion

Here we present the results of the analysis of the external distortion effects for the double isobaric analog transitions for  $^{14}\text{C}$ , i.e. the  $^{14}\text{C}(\pi^+, \pi^-)^{14}\text{O}(\text{DIAS})$  reaction at the pion kinetic energy  $T_\pi = 50$  MeV. We consider here the SEQ mechanism, which has been studied in details in the plane wave approximation in [5].

### 4.1 Distortion Factors

According to Eqs.(25) and (29), we write the distortion factors as a sum of two terms

$$\gamma_\alpha^{DW}(k_f, k_i) = \gamma_\alpha^{DW}(k_f, k_i; \text{on-shell}) + \gamma_\alpha^{DW}(k_f, k_i; \text{off-shell}), \quad (36)$$

where the on-shell distortion factor is expressed in terms of the elastic scattering amplitudes by Eq.(25), the off-shell distortion factor, which is determined by the principal value part of the integral (30), depends, in addition, on the pion-nucleus form factors.

To analyze the effect of distortion it is convenient to represent the distortion factors as

$$\gamma_\alpha^{DW} = |\gamma_\alpha^{DW}|e^{i\phi_\alpha} \quad (37)$$

In the Table we present the numerical results, which demonstrates the contribution to the overall distortion effect of the on- and off-energy shell distortion factors.

The pion-nucleus scattering amplitudes are calculated using the program PIESEX, which is described in [16]. The parameters of the pion-nucleus optical potential [16] and the parameters of the nuclear density Eq.(35) for  $^{14}\text{C}$  also are taken from [16].

The pion-nucleus form factors are calculated for the optical potential Eq.(31), the parameters of which are taken to be

$$\begin{aligned}b_{eff}(fm) &= -0.074 + i0.018 \\ c_{eff}(fm^3) &= 0.427 + i0.040\end{aligned}\quad (38)$$

These values correspond to Set E of the MSU optical potential [18] which provides the best fit of the 50 MeV elastic scattering data for this potential.

Contribution of the on- and off-energy-shell distortion factors to the external pion distortion effect for the separate partial waves. The meaning of the definitions is given in the subsection 4.1.

L	On-shell		Off-shell		Full	
	$ \gamma_{\alpha}^{DW} $	$\phi_{\alpha}[\text{deg.}]$	$ \gamma_{\alpha}^{DW} $	$\phi_{\alpha}[\text{deg.}]$	$ \gamma_{\alpha}^{DW} $	$\phi_{\alpha}[\text{deg.}]$
0	0.694	-23.33	0.187	-61.28	0.849	-31.11
1	0.727	23.07	0.575	60.08	1.236	39.32
2	0.908	14.21	0.951	34.98	1.829	24.84
3	0.992	2.50	0.549	12.91	1.535	6.20
4	0.999	0.26	0.266	6.25	1.264	1.52
5	1.000	0.02	0.134	3.84	1.134	0.47
6	1.000	0.001	0.071	-3.50	1.071	-0.23

The  $\pi$ -nucleus form factors Eq.(33) due to the complex optical potential parameters Eq.(38) are complex. However, in our calculations, we neglected the imaginary parts of the parameters  $b_{eff}$  and  $c_{eff}$ , i.e. we use for R in Eq.(34)

$$R = \alpha \frac{Re c_{eff}}{Re b_{eff}}$$

This approximation is justified by the following reasons. First, from Eq.(34) it follows that the parameter  $\beta_1$  is real for the S-wave, which gives the main contribution to the distortion effect. Second, we estimated the imaginary parts of the parameters  $\beta_{1,2}$  and have found that their imaginary parts are negligible in the low-energy region.

From the Table it is seen that the external distortion strongly influences the angular distribution. The absolute value of the distortion factors (see Eq.(37))  $|\gamma_{\alpha}^{DW}|$  reaches the value  $\sim 2$  for the D-wave decreasing then to unity with increasing of the orbital momentum. The phases  $\phi_{\alpha}$  of the distortion factors also change strongly the plane wave results especially for S- and P-waves.

The results presented in the Table also show that both the on-shell and off-shell distortions are important though the major contribution comes from the on-shell piece.

## 4.2 Distortion effect for SEQ

In Fig.1 we present results of our calculations of the differential cross section for DCX to DIAS for  $^{14}\text{C}$  using  $U_2^{SEQ}$  taken from [5]. The plane-wave result is given by the dashed line. The on-shell external distortion (short-dashed line) decreases substantially the plane wave angular distribution over the whole range of the scattering angles. Turning on the off-shell distortion (solid line) changes qualitatively the plane wave result, increasing it at forward angles and decreasing at large angles. The same qualitative effect of the external distortion has been obtained in [8] (DWIA approximation).

The results in Fig.1 are unrealistic for several reasons. One is that the pion wave internal to the amplitude is taken to be a plane wave in [5]. Thus the calculation in Fig.1 is only meant to illustrate our method and not to be final result. Effects of

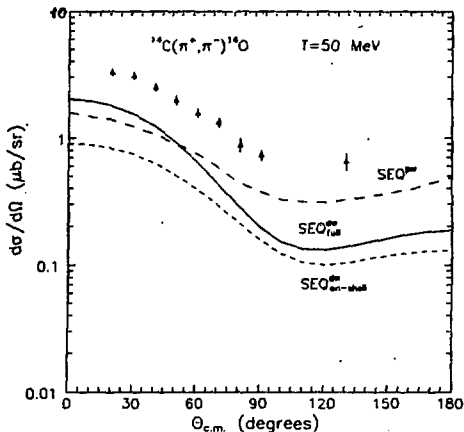


Figure 1: Differential cross sections for DCX  $^{14}\text{C}(\pi^+, \pi^-)^{14}\text{O}$  to DIAS at  $T_\pi = 50\text{ MeV}$ . Calculations have been done for sequential mechanism. Dashed line corresponds to the plane wave results [5], solid line is for full and short-dashed line is only for on-shell external pion distortion calculations. The experimental data are taken from [4].

internal distortion will be considered in a subsequent publication. Secondly, the AR contribution implicit in  $U_2^{SEQ}$  is not realistic, as discussed in Introduction.

The formalism for taking into account the contribution of the AR transitions for the DCX scattering to DIAS (within the framework of the isospin-invariant optical model) has been developed in Subsects. 2.1 and 2.2, where the two-potential formula (14) for DCX amplitude has been derived. For the SEQ mechanism, the isotensor part  $U_2$  of the optical potential, which determines the isotensor amplitude (15), reads as (see Appendix A)

$$U_2 = U_2^{NAR} \equiv U_2^{SEQ} - \Delta U_2^{AR}.$$

Here  $\Delta U_2^{AR}$  is the intermediate state contribution, which is subtracted to avoid double counting. Below we show the contributions of the AR and the isotensor potential  $U_2^{NAR}$  separately. The amplitude corresponding to  $U_2^{NAR}$  we label as  $T_2(NAR)$ , to  $\Delta U_2^{AR}$  as  $T_2(AR)$ , and the AR (which is taken from Ref. [16]) as  $T^{AR}$ .

### 4.3 Analog Route Transition

Consider first the contribution of the AR arising from the lowest-order optical potential (see Eq.(A.5) in Appendix A)

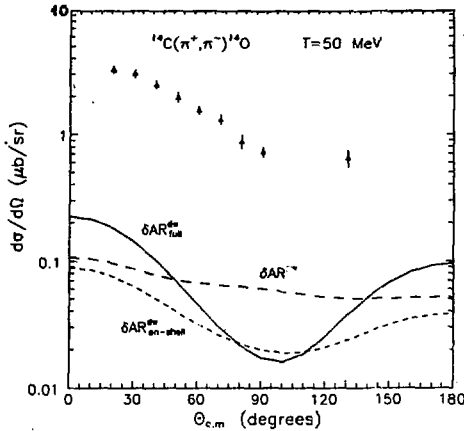


Figure 2: Contribution of analog route to differential cross sections of Fig.1. The meaning of the curves is the same as in Fig.1

The contribution of the AR,

$$T_2(AR) = \langle \psi_{k_f}^{(-)}(\pi^-; DIAS) | \Delta U_2^{AR} | \psi_{k_i}^{(+)}(\pi^+; g.s.) \rangle,$$

to the isotensor potential  $U_2^{SEQ}$  is shown in Fig.2. The dashed line shows the plane-wave approximation. The on-shell external distortions (short-dashed line) decreases substantially the plane-wave angular distribution over the entire range of scattering angles. Turning on the off-shell distortion (solid line) changes qualitatively the plane-wave result, increasing it at forward angles increasing it both at small and large angles, and decreasing at angles around  $90^\circ$ .

In Fig.3 we compare the AR with external distortions (short-dashed line) taken from Fig.2 with the corresponding AR calculation (dashed curve) taken from Ref. [16] (calculated with the lowest-order optical potential  $U_1^{(1)}$ ). This result includes the internal as well as external distortions of the pion, as it results from a full optical potential calculation. We see that the internal distortions, at least for the AR piece of the amplitude, changes drastically the cross section increasing it by an order of magnitude at forward angles.

The lowest-order optical potential does not contain the isovector correlation term (ELIV) which strongly effects on the SCX and DCX cross sections as it has been demonstrated in [16] (see Figs. 3 and 4 therein). The solid curve in Fig.3 shows the result of the optical-model calculation including the full  $U_1$  (including the isovector ELIV term and the second-order isovector absorption-dispersion term of Ref. [16], needed to improve the small angle SCX cross section). We see by comparing the dashed

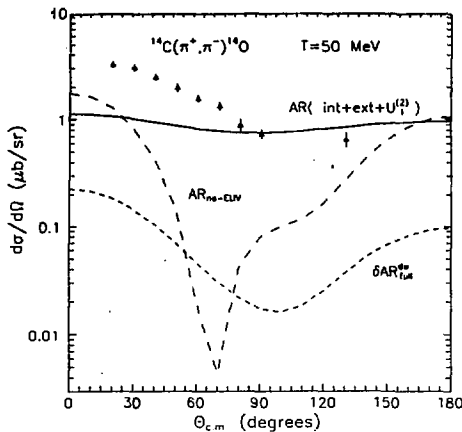


Figure 3: DCX differential cross sections for analog route  $^{14}\text{C}(\pi^+, \pi^-)^{14}\text{O}$  to DIAS at 50 MeV. Solid curve represents the AR transitions calculated within the program PIESEX [16] with the  $U_1^{(2)}$  contribution, dashed curve is the same but without ELIV term of isovector potential, short-dashed curve corresponds to the solid curve of Fig.2.

and solid curves that the second-order isovector effects are very important corrections for the AR.

#### 4.4 Nonanalog Route Transition

In Fig.4 we show the effect of external distortions on  $U_2^{NAR}$ . The plane-wave result is given by the dashed line. The on-shell distortions (short-dashed line) decreases substantially the plane-wave angular distribution over the entire range of scattering angles. Turning on the off-shell distortion (solid line) changes qualitatively the plane-wave result, increasing it at forward angles and decreasing it at large angles. The results are qualitatively similar to the results obtained for cases shown in Fig.1. The difference between the solid line and the long-dashed line (the SEQ with external distortions, taken from Fig.1) shows the AR contribution to the SEQ amplitude.

As we said earlier these results may be changed when the internal distortions of the pion are considered. It will interesting to see whether the internal distortions have as large effect for  $U_2^{NAR}$  as they are in Fig.3 for  $\Delta U_2^{AR}$ .

#### 4.5 Combined results

In Fig.5 we show the analog route contribution as the short-dashed curve (same as in Fig.3) and the nonanalog route contribution as the dashed line (same in Fig.4).

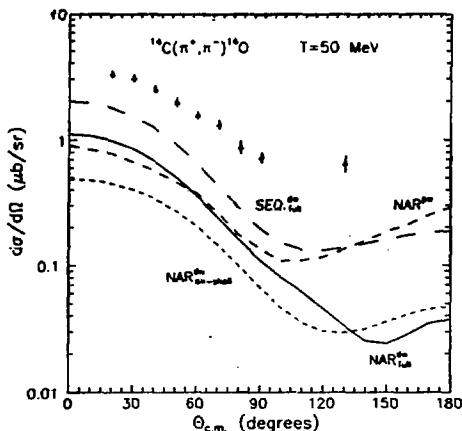


Figure 4: Contribution of nonanalogue route to differential cross sections of Fig.1. The meaning of the curves is the same as in Fig.1. The full distorted wave sequential mechanism resulted in long-dashed curve is also presented.

The combined amplitude (14) is shown as the solid line. We see that the result is comparable to the experimental data throughout the whole angular range.

#### 4.6 Conclusion

The purpose of this paper is to study the role of the external distortion effects in pion-nucleus DCX to DIAS reaction at low energies. The main results could be summarized as following.

We propose an effective method of taking into account the external distortion effects based on the separable approximation of the given optical potential. Due to this method the resulting DW amplitude is given as a product of the plane wave amplitude and the distortion factor, which are expressed in terms of the pion-nucleus form factors. It should be stressed that this method can be also applied to study the effects of external pion distortions in various reaction in which a pion appears in the initial or final states such as in the photo-pion absorption and production reactions, pion absorption processes, etc.

As the particular example of the application of this method we studied the external distortion effect for the sequential mechanism for the DCX to DIAS for. It is shown that the distortion strongly influences the plane wave results increasing the angular distribution at forward angles and decreasing at large angles. The same qualitative effect of the external distortion has been obtained in [8] (DWIA approximation). It is also shown that both the on-shell and off-shell distortion are of an importance.

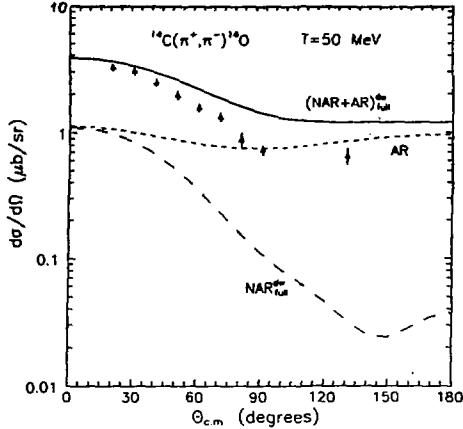


Figure 5: Differential cross sections for DCX  $^{14}\text{C}(\pi^+, \pi^-)^{14}\text{O}$  to DIAS at  $50\text{MeV}$ . Dashed curve represents the distorted wave NAR contribution, short-dashed curve corresponds to the solid curve of Fig.3, solid curve is a summary of given above NAR and AR mechanisms.

We investigated the effect of the analog-route transitions for the DCX to DIAS for  $^{14}\text{C}$  at  $50\text{MeV}$  within the framework of the isospin invariant optical model. The isovector part of the optical potential is fitted to the SCX data. It is shown that the AR contribution to the isotensor  $SEQ - \pi$  amplitude is moderately small (see Fig.4), but the AR-amplitude interferes constructively with the isotensor NAR-amplitude, and the combined result is comparable to the experimental angular distribution.

We also studied the effect of the internal distortion on the AR transitions, and it is shown that this effect strongly changed the cross section calculated in the distorted-wave approximation in which only external distortions are taken into account (see Fig.3). This result indicates an importance of the study of the effect of distortion of the virtual pion in the  $SEQ - \pi$  mechanism. This problem is under investigation now, and the results will be reported in a subsequent publication.

## Acknowledgments

M. Khankhasayev would like to thank the hospitality of the Los Alamos National Laboratory where the work was started; M. B. Johnson, M. Khankhasayev and H. Sarafian the Institute for Nuclear Theory of Seattle where the work was continued; and M. B. Johnson and H. Sarafian the Joint Institute for Nuclear Research where the work was concluded. We are also grateful to V. B. Belyaev for discussions.

## Appendix A

In this paper we have adopted the plane-wave sequential DCX amplitude  $T^{SEQ} \equiv U_2^{SEQ}$  described in Fig.1(a) of Ref. [5] as basis of the isotensor interaction (short-range repulsive correlations acting between the two nucleons are implicit in the figure). This amplitude entails a sum over all intermediate nuclear states, including a piece of  $T^{AR}$  (our Eq.(14)) as taken from Ref. [16]. In order to avoid double counting, we must remove the intermediate analog state contribution

$$\Delta U_2^{AR} = U_1^{(1)} \hat{P}G(E)U_1^{(1)} \quad (A.1)$$

where  $U_1^{(1)}$  is the isovector part of the lowest-order optical potential (1) corresponding to the pion-nucleon scattering amplitude employed in [5]. Therefore, the DCX scattering amplitude is determined now by Eq.(14), where Eq.(15) is replaced by

$$T_2^{DWBA} = \langle \psi_{\vec{k}_f}^{(-)}(\pi^-; DIAS) | U_2^{NAR} | \psi_{\vec{k}_i}^{(+)}(\pi^+; g.s.) \rangle, \quad (A.2)$$

where the isotensor potential  $U_2^{NAR}$  is given by

$$U_2^{NAR} \equiv U_2^{SEQ} - \Delta U_2^{AR}. \quad (A.3)$$

The analog route contribution,  $T^{AR}$ , in Eq.(14) is calculated with the lowest-order isovector optical potential following Ref. [16].

In this Appendix we describe our procedure of calculating the analog route contribution to  $U_2^{SEQ}$ , which in terms of the scattering amplitude reads as

$$\Delta F^{AR} \equiv -\frac{\bar{\omega}}{2\pi} \Delta U_2^{AR}, \quad (A.4)$$

where  $\bar{\omega}$  is the reduced mass of the pion-nucleus system.

To be consistent with the calculation of  $T^{AR}$ , we take the lowest-order optical potential in the following form (compare with Eq.(31))

$$-\frac{2\bar{\omega}}{4\pi} U(r) = b_{eff}^{(1)} \rho(r) - c_{eff}^{(1)} \bar{\nabla} \rho(r) \bar{\nabla} + c_{eff}^{(1)} \frac{\bar{\omega}}{2M} \bar{\nabla}^2 \rho(r), \quad (A.5)$$

where the parameters  $b_{eff}^{(1)}$  and  $c_{eff}^{(1)}$  are determined (see Ref. [16]) as

$$b_{eff}^{(1)} \equiv k^2 \lambda_{s1}^{(1)} / 4\pi A$$

and

$$c_{eff}^{(1)} \equiv \lambda_{p1}^{(1)} / 4\pi A$$

The parameters  $\lambda_{s1}^{(1)}$  and  $\lambda_{p1}^{(1)}$  are related to the single-nucleon parameters  $b_1$  and  $c_1$  of the MSU optical potential [18] as

$$b_1 = \lambda_{s1}^{(1)} (k^2 / 8\pi p_1),$$

$$c_1 = \lambda_{p1}^{(1)} (p_1 / 8\pi),$$

where  $p_1 = (1 + \epsilon)/(1 + \epsilon/A)$ ,  $\epsilon = \omega_\pi/M_N$ ,  $\omega_\pi$  is the pion energy and  $M_N$  is the nucleon mass. In the plane-wave approximation the expression for  $\Delta F^{AR}$  is

$$\langle \vec{k}_f | \Delta F^{AR}(PW) | \vec{k}_i \rangle = -\frac{\bar{\omega}}{2\pi} \int \frac{d\vec{q}}{(2\pi)^3} \langle \vec{k}_f | U_f^{(1)} | \vec{q} \rangle \frac{1}{E(k) - E(q) \pm i\delta} \langle \vec{k}_f | U_f^{(1)} | \vec{k}_i \rangle. \quad (A.6)$$

Decomposing  $\Delta F^{AR}$  into the partial wave series (see Eq.(20)), and using the rank-one separable approximation to the optical potential (A.5) (see Eq.(32) and Appendix B), for a partial wave component we obtain

$$\Delta F_\alpha^{AR}(PW) = -\left(\frac{\bar{\omega}}{2\pi}\right)^2 k U_{1;\alpha}^{(1)}(k_f, k_f) U_{1;\alpha}^{(1)}(k_i, k_i) \xi_\alpha^{(1)}(k_f, k_i), \quad (A.7)$$

where

$$\xi_\alpha^{(1)}(k_f, k_i) = \frac{1}{\pi \epsilon_{\pi A}(k)} \int_0^\infty \frac{q^2 dq}{2\pi^2} \frac{g_\alpha^2(q)}{g_\alpha(k_f) g_\alpha(k_i)} \frac{1}{E(k_i) - E(q) + i\delta}. \quad (A.8)$$

The partial wave components  $U_{1;\alpha}^{(1)}$  of the optical potential (A.1) and the corresponding pion-nucleus form factors  $g_\alpha(k)$  are determined by Eqs. (B.4) and (B.13), where the parameters  $\alpha_i$  are related to the parameters  $b_{eff}^{(1)}$  and  $c_{eff}^{(1)}$  as  $\alpha_1 = b_{eff}^{(1)}$ ,  $\alpha_2 = c_{eff}^{(1)}(\bar{\omega}/2M)$  and  $\alpha_3 = c_{eff}^{(1)}(1 - \bar{\omega}/2M)$ .

To calculate the effect of external distortion of the pion wave we use same procedure as for  $U_2^{SEQ}$  (see Subsections 2.3 - 2.6). Using (28) we obtain

$$\Delta F_\alpha^{AR}(k_f, k_i; DW) = \gamma_\alpha^{DW}(k_f, k_i) \Delta F_\alpha^{AR}(k_f, k_i; PW), \quad (A.9)$$

where the distortion factors  $\gamma_\alpha^{DW}$  are determined in (29).

## Appendix B

In this Appendix we present the procedure of obtaining the pion-nucleus form-factors for a given pion-nucleus potential using Bateman's separable approximation method [22].

The  $\pi$ -nucleus potential (31) in the momentum space is of the form:

$$V(\vec{k}', \vec{k}) \equiv -\frac{2\bar{\omega}}{4\pi} U(\vec{k}', \vec{k}) = \rho(\vec{k}', \vec{k}) [a_1 + a_2(k^2 + k'^2) + a_3(\vec{k}' \cdot \vec{k})], \quad (B.1)$$

where  $a_1 \equiv b_{eff}$ ,  $a_2 \equiv c_{eff}\bar{\omega}/2M$ ,  $a_3 \equiv c_{eff}(1 - \bar{\omega}/2M)$  and

$$\rho(\vec{k}', \vec{k}) = \int d\vec{r} e^{i(\vec{k}' - \vec{k}) \cdot \vec{r}} \rho(r) \quad (B.2)$$

is the nuclear form factor.

Expanding this potential into the partial wave series:

$$V(\vec{k}', \vec{k}) = \sum_{l=0}^{\infty} (2l+1) P_l(\hat{k} \cdot \hat{k}') V_l(k, k') \quad (B.3)$$

we obtain

$$V_l(k', k) = \rho_l(k', k)[a_1 + a_2(k^2 + k'^2)] + \frac{a_3 k k'}{(2l+1)} [l\rho_{l-1}(k', k) + (l+1)\rho_{l+1}(k', k)], \quad (B.4),$$

where

$$\rho_l(k', k) = 4\pi \int_0^\infty dr r^2 \rho(r) j_l(k'r) j_l(kr), \quad (B.5),$$

$j_l(z)$  is the spherical Bessel function.

The Bateman method consists of an approximation of any short-range interaction by the separable potential of the rank-N using the following procedure [22]

$$V_L(k', k) \approx V_L^{(N)}(k', k) = \sum_{i,j=1}^N V_L(k', s_i)(d_L^{-1})_{ij} V_L(s_j, k), \quad (B.6),$$

where  $d_{ij} = V_L(s_i, s_j)$  and  $s_i$  are given values of  $k$  and  $k'$  at which the approximate potential surface  $V_L^{(N)}(k', k)$  coincides with the initial surface  $V_L(k', k)$ .

For the Gaussian type nuclear density

$$\rho(r) = \rho_0(1 + w\alpha r^2) \exp(-\alpha r^2), \quad (B.7),$$

the partial wave component of  $\rho_l(k', k)$  is

$$\rho_l(k', k) = \frac{2\pi^2}{2l+1} \rho_0 \frac{1}{(kk')^{1/2}} D_l(k', k) [1 + w(1 - \frac{kk'}{2\alpha})] + w \frac{kk'}{4\alpha} [D_{l-1}(k', k) + D_{l+1}(k', k)], \quad (B.8),$$

where

$$D_l(k', k) = \frac{1}{2\alpha} \exp[-\frac{k^2 + k'^2}{4\alpha}] I_l(\frac{kk'}{2\alpha}) \quad (B.9),$$

Taking into account that the modified Bessel function  $I_{L+1/2}(z) \sim z^{L+1/2}$  as  $z \rightarrow 0$  one can factorize a trivial power dependence of momenta  $(kk')^L$  in the partial potential  $V_L(k', k)$ , i.e.

$$V_L(k', k) = k'^L k^L \tilde{V}_L(k', k) \quad (B.10),$$

Now the potential  $\tilde{V}_L(k', k)$  has a pronounced bell-like shape for all partial waves. This makes it possible to obtain a good approximation for  $\tilde{V}_L(k', k)$  by the rank-one separable potential [22]

$$\tilde{V}_L(k', k) \approx \tilde{V}_L^{(1)}(k', k) = \lim_{s \rightarrow 0} \tilde{V}_L(k', s) \tilde{V}_L(s, k) / V_L(s, s), \quad (B.11),$$

using the same value of  $s = 0$  for all partial waves.

Using (B.4), (B.8) and (B.10) we obtain the following approximation of the given potential  $\tilde{V}_L(k', k)$ .

$$V_L(k', k) = g_L(k')g_L(k)\gamma_L, \quad (B.12),$$

where the  $\pi$ -nucleus form-factors are of the form

$$g_L(k) = k^L \exp(-z)[1 - \beta_1 z - \beta_2 z^2], \quad z = k^2/4\alpha, \quad (B.13),$$

the strength parameter

$$\gamma_L = \frac{2\pi}{(2L+1)!!} \frac{1}{(2\alpha)^{L+1}} \sqrt{\frac{\pi}{\alpha}} G_L, \quad (B.14),$$

$$G_L \equiv \rho_0 \left[ a_1 \left( 1 + w \frac{2L+3}{2} \right) + 2\alpha a_3 L \left( 1 + w \frac{2L+1}{2} \right) \right],$$

and the parameters  $\beta_1$  and  $\beta_2$  are

$$\beta_1 = [w(1+L\eta) - 4\alpha \frac{a_2}{a_1} (1+w(L+3/2))]/D_L, \quad (B.15),$$

$$\beta_2 = 4\alpha \frac{a_2}{a_1} w/D_L,$$

$$D_L \equiv 1 + L\eta + w(L+3/2) \left( 1 + \frac{L(2L+1)}{2L+3} \eta \right),$$

$$\eta = 2\alpha a_3/a_1$$

Here  $a_1$ ,  $a_2$  and  $a_3$  are the parameters of the optical potential (see Eq.(B.1)), and  $\rho_0$ ,  $w$  and  $\alpha = 1/a^2$  are the parameters of the nuclear density.

## References

- [1] J. Navon et al., Phys. Rev. Lett. 52(1984)105
- [2] A. Altman et al., Phys. Rev. Lett. 55(1985)1273
- [3] M.J. Leitch et al., Phys. Rev. Lett. 54(1984)14824
- [4] M.J. Leitch et al., Phys. Rev. C39(1989)2356
- [5] E.R. Siciliano, M.B. Johnson and H. Sarafian, Ann. of Phys. 203(1990)1
- [6] T. Karapiperis and M. Kobayashi, Phys. Rev. Lett. 54(1985)1230
- [7] M. Bleszynsky and G.J. Glauber, Phys. Rev. C26(1987)681
- [8] Q. Haider and L.C. Liu, Z. Phys. A335(1990)437
- [9] Q. Haider and L.C. Liu, J. Phys. G14(1988)1527; G15(1989)934
- [10] D.S. Koltun and M.S. Singham, Phys. Rev. C419(1990)2266
- [11] E. Oset, M.Kh. Khankhasayev, J. Nieves, H. Sarafian and M.J. Vicente-Vacas (Subm. to Phys. Rev. C)

- [12] M.B. Johnson, E. Oset, H. Sarafian, E.R. Siciliano, M.J. Vicente-Vacas, *Phys. Rev. C*44(1991)2480
- [13] M.F. Jiang and D.S. Koltun, *Phys. Rev. C*42(1990)2662
- [14] M.B. Johnson, *Phys. Rev. C*22(1980)192
- [15] M.B. Johnson and E.R. Siciliano, *Phys. Rev. C*27(1983)730
- [16] E.R. Siciliano, M.D. Cooper, M.J. Johnson and M.J. Leitch, *Phys. Rev. C*34(1986)267
- [17] M.L. Goldberger and K.M. Watson, *Collision Theory*, Wiley, New-York, 1964
- [18] K. Stricker, H. McManus and J.A. Carr, *Phys. Rev. C*19(1979)929; *C*22(1980)2043  
J.A. Carr, H. McManus and K. Stricker, *Phys. Rev. C*25(1982)952
- [19] R. Seki, K. Masutani, M. Oka and K. Yazaki, *Phys. Lett. B*97(1980)200  
R. Seki and K. Masutani, *Phys. Rev. C*27(1983)2799  
R. Seki, K. Masutani and K. Yazaki, *Phys. Rev. C*27(1983)2817
- [20] O. Meirav, E. Friedman, A. Altman, M. Mannach, R.R. Johnson and D.R. Gill, *Phys. Lett. B*199(1987)5
- [21] M.Kh. Khankhasayev and N.S. Topilskaya, *Phys. Lett. B*217(1989)14
- [22] V.B. Belyaev, *Lectures on the Theory of Few-Body Systems*, Springer Series in Nuclear and Particle Physics, Springer-Verlag, Berlin, 1990

Received by Publishing Department  
on March 3, 1993.

## **SUBJECT CATEGORIES OF THE JINR PUBLICATIONS**

<b>Index</b>	<b>Subject</b>
1.	High energy experimental physics
2.	High energy theoretical physics
3.	Low energy experimental physics
4.	Low energy theoretical physics
5.	Mathematics
6.	Nuclear spectroscopy and radiochemistry
7.	Heavy ion physics
8.	Cryogenics
9.	Accelerators
10.	Automatization of data processing
11.	Computing mathematics and technique
12.	Chemistry
13.	Experimental techniques and methods
14.	Solid state physics. Liquids
15.	Experimental physics of nuclear reactions at low energies
16.	Health physics. Shieldings
17.	Theory of condensed matter
18.	Applied researches
19.	Biophysics

Ханхасаев М.Х. и др.

E4-93-60

Роль внешнего искажения пионов  
в реакции двойной перезарядки при низких энергиях

Рассмотрена роль внешнего искажения пионов при изоупругом рассеянии с перезарядкой (в рамках изоспин-инвариантной оптической модели). Разработан метод учета пионного искажения, основанный на приближении сепарабельного разложения оптического потенциала в импульсном пространстве. Данный метод обеспечивает простую процедуру расчета эффектов искажения для однократной и двойной перезарядки пионов в изоупругих каналах рассеяния. Наш подход позволяет проанализировать роль искажения пионов на энергетической и внеэнергетической поверхности для данного парциального канала. Представлен результат расчета внешнего искажения пионов для механизма последовательного рассеяния в реакции  $^{14}\text{C}(\mu^+, \pi^-)^{14}\text{O}$  при 50 МэВ. Показано, что данное искажение приводит к небольшому увеличению дифференциального сечения при малых углах и уменьшению при больших углах рассеяния.

Работа выполнена в Лаборатории теоретической физики ОИЯИ.

Препринт Объединенного института ядерных исследований. Дубна, 1993

Khankhasayev M.Kh. et al.

E4-93-60

Effect of Pion External Distortion  
on Low Energy Pion Double-Charge-Exchange

The effects of the external pion distortion for isoelastic charge exchange scattering (within the framework of the isospin invariant optical model) is considered. An approximated method of taking into account the distortion based on the separable expansion of the optical potential in momentum space is developed. This method provides a simple procedure to calculate the distortion effects for SCX and DCX pion isoelastic scattering channels. Our approach makes it possible to analyze the role of on- and off-shell pions for the given partial wave channels. The result of external distortions for sequential scattering  $^{14}\text{C}(\pi^+, \pi^-)^{14}\text{O}$  at 50 MeV is presented. It is shown that this distortion gives a small enhancement to forward and reduces the differential cross sections at large angles.

The investigation has been performed at the Laboratory of Theoretical Physics, JINR.

Preprint of the Joint Institute for Nuclear Research. Dubna, 1993

23 р. 40 к.

Корректурa и макет Т.Е.Попеко.

Подписано в печать 23.03.93.

Формат 60x90/16. Офсетная печать. Уч.-изд.листов 1,67.

Тираж 380. Заказ 46202.

Издательский отдел Объединенного института ядерных исследований.  
Дубна Московской области.